ACS APPLIED MATERIALS & INTERFACES

Letter

www.acsami.org

Templated Homoepitaxial Growth with Atomic Layer Deposition of Single-Crystal Anatase (101) and Rutile (110) TiO_2

Theodore J. Kraus, Alexander B. Nepomnyashchii, and B. A. Parkinson*

Department of Chemistry, School of Energy Resources, University of Wyoming, Laramie, Wyoming 82071, United States

Supporting Information

ABSTRACT: Homoepitaxial growth of highly ordered and pure layers of rutile on rutile crystal substrates and anatase on anatase crystal substrates using atomic layer deposition (ALD) is reported. The epilayers grow in a layer-by-layer fashion at low deposition temperatures but are still not well ordered on rutile. Subsequent annealing at higher temperatures produces highly ordered, terraced rutile surfaces that in many cases have fewer electrically active defects than the substrate crystal. The anatase epitaxial layers, grown at 250 °C, have much fewer electrically active defects than the rather impure bulk crystals. Annealing the epilayers at higher temperatures increased band gap photocurrents in both anatase and rutile.

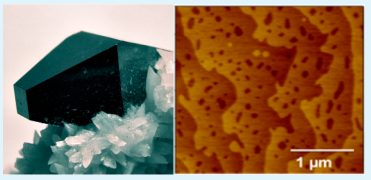

KEYWORDS: *photoactivity, low-temperature deposition, annealing, defects, atomic force microscopy*

Atomic layer deposition (ALD) is a powerful, low-pressure vapor deposition technique of increasing interest in industrial applications, particularly semiconductor processing.[1−3] ALD has the ability to produce highly conformal, pinhole free thin films on high-aspect-ratio surfaces.[2] Although polycrystalline layers have been routinely grown, to the best of our knowledge ALD has not been applied to the growth of homoepitaxial layers of rutile and anatase TiO_2.[1−3] Techniques such as molecular beam epitaxy (MBE) and pulsed laser deposition (PLD) have already been successfully used to grow homoepitaxial layers on rutile and anatase TiO_2 surfaces but are often more expensive and less flexible than ALD.[4,5] Homoepitaxy is widely used in the semiconductor industry to produce the highest performance devices because even the available large high-quality III−V or Si crystals do not have the purity or low defect densities necessary for devices that require high carrier mobilities.[6] Thermodynamic native defects, such as vacancies, are always present in crystals grown near equilibrium at the high temperatures needed for growth from the melt.

High-temperature defects would be expected to be more problematic for oxide single crystals that are often grown at temperatures in excess of 1300−1800 °C.[7,8] Therefore, we decided to investigate the ability of ALD to grow homoepitaxial layers on rutile and anatase TiO_2 crystals at lower temperatures. Synthetic melt-grown rutile (melting point 1843 °C) crystals are often contaminated with elements from the growth crucibles or other materials that contact the growing crystal at such high temperatures. Techniques to grow large synthetic anatase crystals have not been developed, but naturally occurring anatase crystals that likely grew under hydrothermal conditions have been used by our group to investigate fundamental processes in photoelectrochemical energy conversion, such as dye and quantum dot photosensitization of large-band-gap semiconducting oxides.[9−13] Nevertheless, the purity, perfection, and doping densities of the natural crystals are uncontrolled, often resulting in sorting through many natural crystals to find suitable doping densities and/or surface properties. However, the lower-temperature ALD growth conditions, use of highly pure precursors, layer-by-layer control of deposition, and ability to control the location and amounts of dopants may result in superior electronic properties for epilayers.

The precise control of the epilayer growth would allow for the control of space charge layer thickness and the electric field gradients that are important for the collection of photogenerated carriers regardless of their origin, either injected from a sensitizing species or direct band gap photoexcitation in photoconversion devices.

ALD layers were deposited, using 99.99% purity $TiCl_4$ and 18 MΩ water as precursors, on a flat rutile TiO_2 (110) substrate with terrace widths in some areas of hundreds of nanometers as shown in the AFM image in Figure 1a. An AFM image of the same crystal after ALD of 20 nm (∼32 unit cells in the (110) direction) of TiO_2 at a 250 °C substrate temperature is shown in Figure 1b. The terraced structure remains, but the terraces are not as smooth as the substrate and show fingering. Subsequent annealing of the crystal in air for 1 h at 600 °C results in the coalescence of the fingers into more compact smooth terraces as seen in Figure 1c where there are still some small islands of TiO_2 on the terraces. A further hour of annealing at 600 °C continues to coalesce the terraces leaving some pits, as seen in Figure 1d, that presumably would disappear with further annealing. Low-angle X-ray diffraction indicates that the rutile form of TiO_2 is templated at these low temperatures despite the fact that rutile is the high-temperature form of TiO_2.

We also attempted ALD homoepitaxy on natural anatase crystal substrates because it is especially desirable to produce

Received: May 14, 2014
Accepted: June 13, 2014
Published: June 13, 2014

   dx.doi.org/10.1021/am5029507 | ACS Appl. Mater. Interfaces 2014, 6, 9946−9949

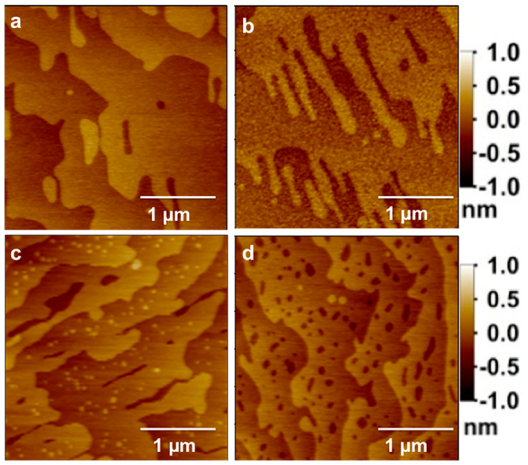

Figure 1. AFM images of a rutile TiO_2 (110) rutile single crystal: (a) prior to deposition; (b) after 20 nm of TiO_2 deposition; (c) after 1 h annealing at 600 °C; (d) after an additional 1 h at 600 °C.

higher-purity anatase surface layers, and to be able to control any impurities that may influence the doping level and carrier mobilities. Epilayers on natural anatase crystals would be especially useful because large synthetic crystals are not commercially available and natural anatase has high levels of impurities that can be detected by XPS as well as lower levels of electrically active impurities acting as n-type dopants. Figure 2a

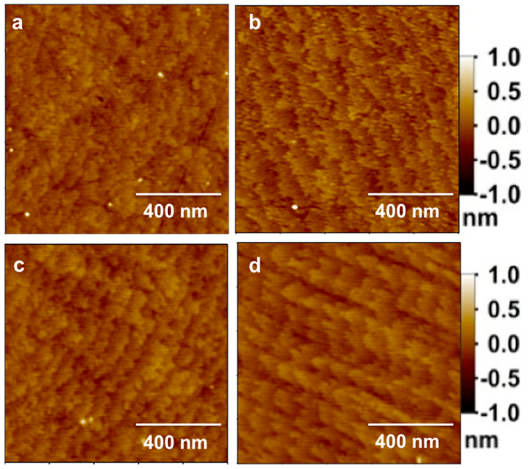

Figure 2. AFM images of an anatase TiO_2 (101) natural crystal: (a) as prepared; (b) after 5 nm of TiO_2 deposition; (c) after 20 nm of TiO_2 deposition; (d) after annealing of the 20 nm film for 2 h.

shows an AFM image of a typical region of a polished and annealed anatase (101) surface showing small ragged terraces <100 nm in width. Depositing 5 nm of TiO_2 resulted in a similar terraced morphology that is maintained after 15 nm (Figure 2b, c) of additional titanium dioxide deposition (~28 unit cells of the 101 plane). Subsequent annealing for 2 h at 350 °C results in a decrease of surface roughness and coalescence of the fingers (Figure 2d), similar as to what is observed on rutile TiO_2 (110). Low-angle X-ray diffraction indicated that the epilayers were anatase again template by the substrate crystal. Silicon, a nonelectrical active impurity, is usually observed in XPS spectra of natural anatase because it is naturally abundant and hydrothermally grown anatase crystals are often found with quartz. XPS analysis of the epilayers did not show any SiO_2 impurity, as was detected on the natural anatase crystal prior to deposition, indicating that a higher-purity anatase layer was prepared (see Figure S2 in the Supporting Information).

To further ascertain the purity and level of electrically active impurities, weperformed Mott–Schottky analysis on electrodes with epilayers prepared on a rutile TiO_2 (110) substrate that was highly doped by heating in vacuum according to the experimental procedure described in the Supporting Information.

Figure 3a shows the doping density, determined from the slope of the nicely linear Mott–Schottky plots, increased from

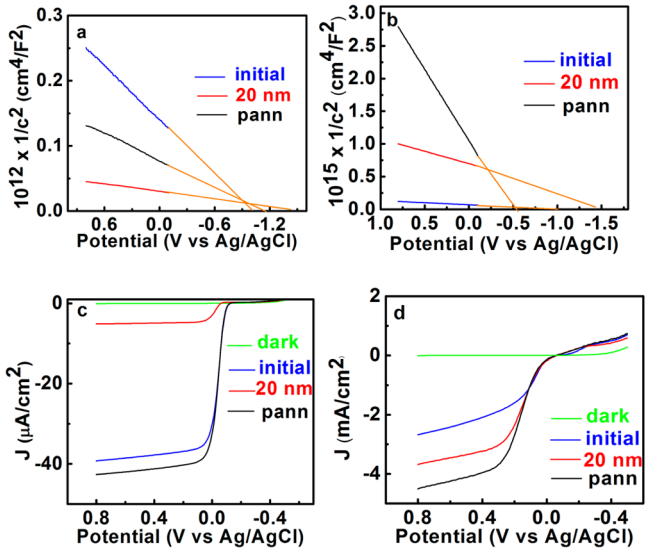

Figure 3. Mott–Schottky plots for a) rutile (110) and b) anatase (101) TiO_2 single crystals: prior to deposition (blue lines), after 20 nm of ALD (red lines) and after post-deposition annealing in vacuum (black lines). The orange lines are an extrapolation to determine the flat band potentials. Voltammetric (I–V) curves for (c) rutile and (d) anatase, where the green and blue lines are the dark current and photocurrent, respectively, for the substrate crystals and red and black are the photocurrent responses after 20 nm of ALD before and after annealing, respectively, with 370 nm LED illumination for rutile and arc lamp illumination for anatase.

2.5×10^{18} cm^{-3} to 2.1×10^{20} cm^{-3} in the epilayer after deposition of a 20 nm ALD TiO_2 layer.[14] Subsequent annealing in vacuum decreased the doping density from 2.1×10^{20} cm^{-3} down to 2.8×10^{19} cm^{-3}. The AFM results showed nicely formed terraces indicating the surface area of the crystal was not substantially changed by the epilayer growth and annealing. However, some of the decrease in apparent doping density could be caused by annealing out the surface roughness like that shown in Figure 1b prior to annealing (see Figure S1b in the Supporting Information). After a 20 nm deposition, anatase exhibits a different behavior with a decrease of the doping density from 3.9×10^{20} cm^{-3} to 6.4×10^{19} cm^{-3} even without annealing with a further decrease to 1.1×10^{19} cm^{-3} with air annealing (Figure 3b). The identity of the electrically active dopants in the annealed samples is not known but could be due to residual chloride from the $TiCl_4$ precursor on oxygen lattice sites at levels not detected by XPS analysis. Previous reports of pulsed laser deposition (PLD) of homoepitaxial layers of TiO_2 onto Nb-doped TiO_2 substrates resulted in an increase in the doping density.[15]

dx.doi.org/10.1021/am5029507 | ACS Appl. Mater. Interfaces 2014, 6, 9946–9949

The apparent flat band potentials, for both anatase and rutile crystals with as deposited ALD layers, also substantially shifted from values of around −1.0 to −1.5 V for rutile and from around −1.2 V to −1.4 V for anatase. Annealing shifts the flat band potential back to less negative potentials (−1.2 V for rutile and −0.5 V for anatase) perhaps due to removal of charged impurities or defects.

Dark and photocurrent voltage curves for the rutile crystals with and without a 20 nm epilayer are shown in Figure 3c. The TiO_2 substrate crystal shows a typical sigmoidal photocurrent voltage curve for oxygen evolution with a plateau current of around 38 $\mu A/cm^2$ under illumination with 60 μW of 370 nm from a UV-LED. The photocurrent decreased from 38 $\mu A/cm^2$ before deposition to 5 $\mu A/cm^2$ after deposition. Vacuum annealing of the epilayers resulted in the recovery of the photocurrent to a value of 42 $\mu A/cm^2$. Current−voltage curves for anatase were measured using an arc lamp since the 370 nm UV-LED is just below the anatase band gap (Figure 3d). Unlike rutile the photocurrent increased after both deposition and air annealing. The upward slope in the plateau region of the photocurrent voltage curve indicates that photogenerated carriers are primary being collected from the space charged layer at the semiconductor/electrolyte interface.

IPCE spectra (Figure 4a), for a 20 nm epilayer on a rutile crystal, shows a decrease of the photocurrent at all wavelengths

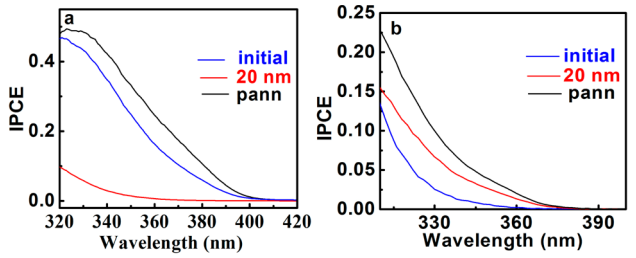

Figure 4. IPCE spectra for (a) rutile (110) and (b) anatase (101) TiO_2 single crystals: initial response (blue), after 20 nm of ALD (red), and after annealing the ALD film in vacuum (black) for rutile and in air for anatase.

compared to the initial vacuum doped crystal but IPCE increases at all wavelengths after vacuum annealing. The photocurrent response for epilayers was more reproducible than on the vacuum doped substrate crystals (see Figure S3 in the Supporting Information). The calculated width of the space charge layers at the measured doping densities is 10−15 nm for the doped and annealed samples compared with the penetration depth of the 370 nm illumination of 20−50 nm; however, the light penetration depth is substantially less at shorter wavelengths.[16,17] Photocurrent, Mott−Schottky and IPCE results with 40 nm epilayers on rutile are similar to those from the 20 nm layers (see Figure S3 in the Supporting Information).

The anatase showed increases in IPCE at all wavelengths both immediately after deposition as well as with air annealing (Figure 4b) as was also seen in the *I*−*V* curves. The photocurrent increase on unannealed layers may be due the ALD growth occurring at temperatures similar to those for growth of natural anatase crystals, the stable low-temperature form of TiO_2, albeit with much fewer impurities present. The highly doped natural substrate crystal is also much more conductive reducing the resistance to current flow through the bulk crystal and providing a good contact to the epilayer.

In summary, we have shown that ALD can produce pure and highly ordered homoepitaxial layers on both rutile and anatase crystals. The reproducibility of the epilayers, when compared to the variation in substrate crystal quality and impurity levels, makes these epilayer films attractive for fundamental studies of these materials especially in the case of anatase. where high-quality synthetic single crystals are not commercially available but the naturally occurring crystals provide an excellent substrate.

■ ASSOCIATED CONTENT

Supporting Information

Experimental details and characterization data such as XPS, additional AFM images, and photoelectrochemical data. This material is available free of charge via the Internet at http://pubs.acs.org.

■ AUTHOR INFORMATION

Corresponding Author

*E-mail: bparkin1@uwyo.edu.

Notes

The authors declare no competing financial interest.

■ ACKNOWLEDGMENTS

We acknowledge Dr. Erwin Sabio for his assistance in obtaining XPS results and J. Conrad Vogel P.E. for ALD engineering support and photoelectrochemical cell development. This work was funded by the Division of Chemical Sciences, Geosciences, and Biosciences, Office of Basic Energy Sciences of the U.S. Department of Energy, through Grant DE-FG02-05ER15750. T.J.K. also thanks the National Science Foundation and University of Wyoming EE-Nanotechnology Program (NSF-40243) for a fellowship.

■ REFERENCES

(1) Suntola, T. Atomic Layer Epitaxy. *Thin Solids Films* **1992**, *216*, 84−89.

(2) George, S. M. Atomic Layer Deposition: An Overview. *Chem. Rev.* **2010**, *110*, 111−131.

(3) Mikkulainen, V.; Leskela, M.; Ritala, M.; Purrinen, R. L. Crystallinity of Inorganic Films Grown by Atomic Layer Deposition: Overview and General Trends. *J. Appl. Phys.* **2013**, *113*, 021301/1−021301/101.

(4) Yamamoto, Y.; Matsumoto, Y.; Koinuma, H. Homo-epitaxial Growth of Rutile TiO_2 on Step and Terrace Structured Substrate. *Appl. Surf. Sci.* **2004**, *238*, 189−192.

(5) Herman, G. S.; Gao, Y. Growth of Epitaxial Anatase (001) and (101) Films. *Thin Solid Films* **2001**, *397*, 157−161.

(6) Tu, K.-N.; Mayer, J. W.; Feldman, L. C. *Electronic Thin Film Science for Electrical Engineers and Materials Scientists*; Macmillan: New York, 1992; pp 127−157.

(7) Chase, J. D.; Van Ruuyven, L. J. Plasma-Grown Rutile Single Crystals and Their Distinctive Properties. *J. Cryst. Growth* **1969**, *5*, 294−298.

(8) De La Rue, R. E.; Halden, F. A. Arc-Image Furnace for Growth of Single Crystals. *Rev. Sci. Instrum.* **1960**, *31*, 35−38.

(9) Kavan, L.; Grätzel, M.; Gilbert, S. E.; Klemenz, C.; Scheel, H. J. Electrochemical and Photoelectrochemical Investigation of Single-Crystal Anatase. *J. Am. Chem. Soc.* **1996**, *118*, 6716−6723.

(10) Ushiroda, S.; Ruzycki, N.; Lu, Y.; Spitler, M. T.; Parkinson, B. A. Dye Sensitization of Anatase (101) Crystal Surface by a Series of Dicarboxylated Thiacyanine Dyes. *J. Am. Chem. Soc.* **2005**, *127*, 5158−5168.

(11) Lu, Y.; Choi, D.-J.; Nelson, J.; Yang, O.-B.; Parkinson, B. A. Adsorption, Desorption and Sensitization of Low-Index Anatase and

Rutile Surfaces by the Ruthenium Complex Dye N3. *J. Electrochem. Soc.* **2006**, *153*, E131−E137.
(12) Sambur, J. B.; Novet, T.; Parkinson, B. A. Multiple Exciton Collection in a Sensitized Photovoltaic System. *Science* **2010**, *330*, 63−66.
(13) Choi, D.-J.; Rowley, J. G.; Spitler, M.; Parkinson, B. A. Dye Sensitization of Four Low Index TiO_2 Single Crystal Photoelectrodes with a Series of Dicarboxylated Cyanine Dyes. *Langmuir* **2013**, *29*, 9410−9419.
(14) Cooper, G.; Turner, J. A.; Nozik, A. J. Mott-Schottky Plots and Flatband Potentials for Single Crystal Rutile Electrodes. *J. Electrochem. Soc.* **1982**, *129*, 1973−1977.
(15) Takata, S.; Tanaka, R.; Hachiya, A.; Matsumoto, Y. J. Nanoscale Oxygen Nonstoichiometry in Epitaxial TiO2 Films Grown by Laser Pulsed Deposition. *J. Appl. Phys.* **2011**, *110*, 103513/1−103513/5.
(16) Cronemeyer, D. C. Electrical and Optical Properties of Rutile Single Crystals. *Phys. Rev.* **1952**, *87*, 876−886.
(17) Krool, V. D., Grätzel, M., Eds.; *Photoelectrochemical Hydrogen Production*; Springer: New York, 2012; p 324.